Measuring the Separation and Position Angle of Two Double Stars: STF 1169 AB and STF 42 AB

Researchers have been observing multiple star systems for centuries in the hopes of understanding them more and calculating their orbits. Our paper aimed to add to the historical data of two binary stars, STF 1169 AB and STF 42 AB, by measuring their separation and position angle. The values measured for STF 1169 AB were 20.94 *arcsec* and 15.46°, while the values for STF 42 AB were 6.26 *arcsec* and 20.41° .

PACS numbers: 06.30.-k,42.25.Bs

I. INTRODUCTION

Although the idea of a double star was first proposed in the 2nd century AD, these stellar objects were not observed until much later with the invention of the telescope in 1608 [9][7]. The first binary star system – now known as Mizar – was discovered in 1650 by Giovanni Battista Riccioli, with many more observed after. These discoveries were eventually collected by Christian Mayer in 1779 who then compiled them into the first double star catalogue [9].

Our modern understanding of binary stars didn't begin to take shape, though, until the publication of Sir William Herschel's discoveries in 1802 [1]. Since then Astronomers have continued to observe double star systems in order to understand them better and discover if they are in fact true binaries. One way this is accomplished is through measuring the separation between the A and B stars of the system and the position angle of the B star relative to the A star; these values function as the ρ and θ attributed to polar coordinates and, after measuring these values over several years, can be used to create an estimated orbit of the B star around the A star. Continued observations allow astronomers to further refine this estimation or declassify the star as a binary if the A and B stars appear to be drifting apart [10]. The goal of this project was to create new data for two double stars, STF 1169 AB and STF 42 AB, in order to help future astronomers make better estimated orbits and to better our understanding of these two systems.

STF 1169 (WDS 08165+7930) is a 3 star system located in the Camelopardalis constellation and is classified as a physical double. It was first observed by Friedrich Georg Wilhelm von Struve in 1932; the third star (C) in the system was not discovered until 1962, though [13]. This paper focuses on the analysis of the A and B stars only. The orbit of this binary was first estimated by Kisselev, et al. in 2009 but, due to the stars large estimated orbital period of 200 centuries, STF 1169 is considered a Short-Arc Binary. Short-Arc Binaries are labeled as such since their data has been collected for such a relatively short period of time that the data only spans a small arc of the stars orbit; this makes it especially difficult for astronomers to estimate the orbit and for this orbit to be taken as a good approximation. Continuing to measure the separation and position angle is the only way to increase the accuracy of the estimated orbits of Short-Arc Binaries [4][13]. The current estimated orbit is shown in Figure 1. Our measurements of STF 1169 AB are meant to aid in the process of making this plot more accurate.

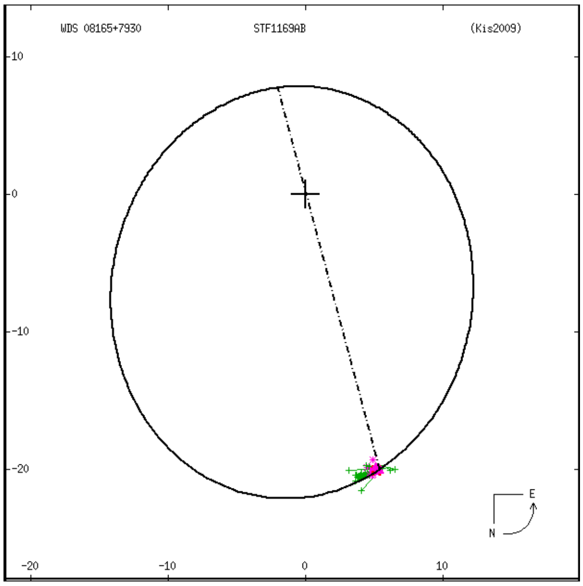

FIG. 1: The estimated orbital plot of STF 1169 AB calculated by Kisselev, et al. The historical data of STF 1169 AB is represented by the multicolored dots along the orbit; two colors were used, green and pink, and represent data taken through micrometric and photographic processes respectively.

STF 42 (WDS 00360+2959) is also a 3 star, physical system and, as with STF 1169, this paper only discusses the A and B stars. This binary is located in the Andromeda constellation and is part of the Arcturus moving group; it is also classified as a sub-dwarf triple system [6][14]. The first estimated orbit for STF 42 AB was made as a single-lined orbit in 1988 by Latham, et al. and has a period of approximately $1,900$ years [12]. Since then, two more orbits have been calculated for STF 42 AB, one in 2009 and the other more recently in 2019. Both of these orbits are considered as potentially accurate and it is still up for debate on which one is correct; these orbits can be seen in Figure 2. Although the period is not as large as that of STF 1169 AB, STF 42 AB is still considered a Short-Arc Binary since data for it has been collected over a relatively short amount of time compared to its orbital period; the arc created by the current data is much smaller than the estimated orbit. Therefore, we approached our measurements of STF 42 AB in the same way as STf 1169 AB: with the intent of creating a larger data set for the binary star in order for future astronomers to create more accurate orbits.

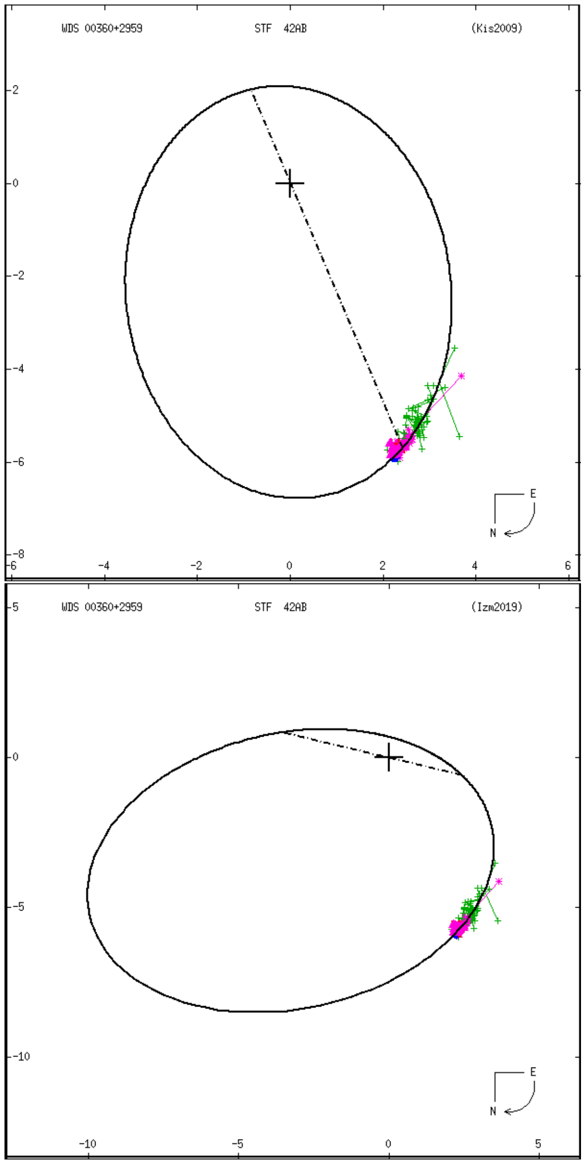

FIG. 2: Two potential orbits for STF 42 AB. The top orbit was made in 2009 by Kisselev, et al.; the bottom orbit was calculated in 2019 by Ismailov, et al. In both plots the pink dots represent measurements made photographically, the blue dots were made interferometrically, and the green dots were made micrometrically.

II. METHODS

In order to measure the separation and position angle, we chose to use the photographic method, which involves taking images of a double star and then measuring the separation and position angle directly from the image. Our images were taken using the Las Cumbres Observatory (LCO), a global network of 25 telescopes; the specific telescopes used were the 0.4 m telescopes located in Spain, Texas, and Hawaii. The LCO's 0.4 m telescopes are heavily modified Meade 16 in telescopes and are equipped with an SBIG STL-6303 CCD camera, which can be seen in Figure 3 [3].

When selecting which double stars to observe, two criteria were considered: the magnitudes of the A and B stars and their previously calculated separation. In order for the telescope to be able to take images of our double stars, the A and B stars must have magnitudes between 7 and 10; magnitudes less than 7 would likely be too bright while magnitudes greater than 10 would be too faint. On top of this, the separation must be large enough such that the two stars do not overlap. If one or both stars are too bright and have too small of a separation, the individual stars cannot be resolved, making measurements of their current separation and position angle impossible. Initially, any binary with a separation greater than 3 $arcsecs$ was considered but this was eventually determined to be too small for stars closer to magnitudes of 7, so this lower limit was changed to 5 or 6 $arcsec$. To be extra careful, only magnitudes of 8 or greater were consider instead of magnitudes closer to 7. The two stars that met these requirements – and were visible during the time of this project – were STF 1169 AB and STF 42 AB.

STF 42 AB has a primary magnitude of 8.39, a secondary magnitude of 9.05, and a most recent separation of 6.037 $arcsec$. This binary was selected for its relatively low magnitudes and large separation compared to the other stars we had to choose from. STF 1169 AB has a primary magnitude of 8.4 and a secondary magnitude 8.64. It's last measured separation is 20.56 $arcsec$. We

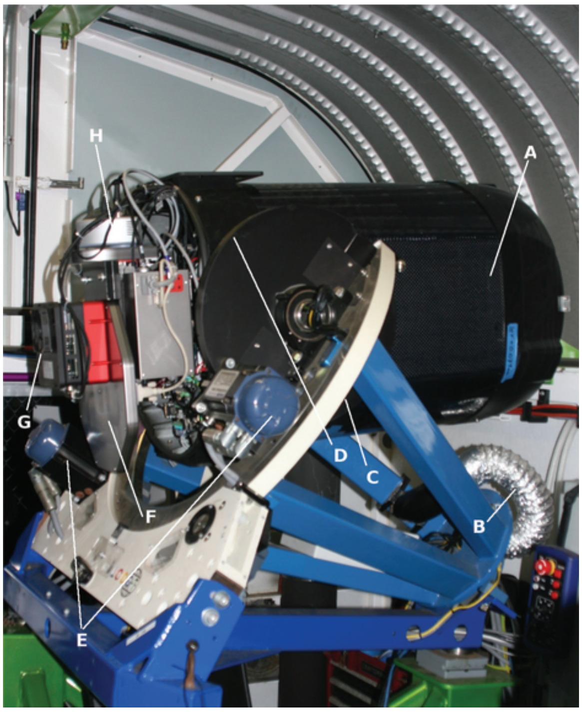

FIG. 3: The LCO's 0.4 m telescope. The component labelled G is the SBIG STL-6303 CCD camera that we used to take our images [3].

initially chose STF 1169 AB as a back-up for if the stars of STF 42 AB were too close and too bright; STF 1169 AB's large separation was the primary factor in this decision, as we knew the A and B stars would not overlap with each other, but we did not choose it as our first subject of observation since we were not sure if this separation would be too big. After receiving the images from the LCO and seeing that both stars were measurable, we decided to make measurements for STF 42 AB and STF 1169 AB.

For each double star, 60 images were taken in total, with 15 images in each of the following filters: Bessel B, Bessel V, SDSS r', and SDSS i'. We chose an exposure time of 1 s and determined the signal to noise ration for both stars in each filter. The equation for the signal to noise ratio is,

$$\frac{S}{N} = \frac{FA_{\varepsilon}\tau}{\sqrt{{N_R}^2 + \tau N_T}} \tag{1}$$

where F is the point source signal flux on the telescope, A_{ε} is the effective area, τ is the integration (exposure) time, N_R is the readout noise, and N_T is the time-dependent noise per unit time. N_R is a constant – in this case it is 14 e^- – whereas all other values in the above list can be calculated through various equations, as discussed below.

Values of Variables	
Symbol	value
Q_e	0.2
N_R	14 e^-
Ω	0.571 arcsec
i_{DC}	0.02 $\frac{e^-}{s}$
A	1200 cm^2
ε	0.5
F_β	0.1 $\frac{photon}{s \cdot cm^2}$

TABLE I: The various constants used to calculate A_{ε}, N_T, and the signal to noise ratio. These values are based on the telescope used for the observations.

The point source signal flux depends on both the magnitude of the object and the filter it was observed in and can be found using Equation 2.

$$F = 10^{-0.4M} F_o \left(\frac{d\lambda}{\lambda}\right) \cdot \left(1.51x10^7 \frac{photons}{m^2 \cdot s \cdot Jy}\right)\left(\frac{m^2}{100^2 cm^2}\right) \tag{2}$$

In the first part of Equation 2, M is the magnitude of the observed object, F_o is the flux of an object with magnitude 0 for a given filter, and $\frac{d\lambda}{\lambda}$ is the filter bandpass; this part of the equation calculates the desired flux for a given M, while the rest of the equation converts it to the desired untis, $\frac{photons}{cm^2 \cdot s}$. In our calculations of F, the magnitude of the fainter star was used so as to ensure that the fainter star would be visible in our images (9.05 for STF 42 AB and 8.64 for STF 1169 AB). The values for F can be found in Table II [15].

The effective area, A_{ε}, and time-dependent noise per unit time, N_T, are calculated using properties of the telescope, with N_T also being dependent on A_{ε} and F. The expressions for these values are as follows:

$$A_{\varepsilon} = A\varepsilon Q_e \tag{3}$$

$$N_T = FA_{\varepsilon} + i_{DC} + F_\beta A_{\varepsilon}\Omega \tag{4}$$

In Equation 3, ε and Q_e are the telescope and quantum efficiencies respectively. The variables in Equation 4 are the dark current (i_{DC}), the background flux (F_β), and the pixel size (Ω). These values can be found in Table I.

After A_{ε} and N_T were calculated, we used Equation 1 to calculate the signal to noise ratios for both stars; the signal to noise ratio for each filter can be found in Table II. Since all of them were above or near 150, we decided that 1 s would be an appropriate exposure time for our observations.

Once the images had been received, they were processed in AstroImageJ, a common program used in the

Signal to Noise Ratios for STF 1169 and STF 42			
Star	Filter	Flux ($\frac{photons}{cm^2 \cdot s}$)	S/N
1169	V	307.75	191.6
1169	B	495.23	243.4
1169	i	402.44	219.3
1169	r	332.16	199.1
42	V	210.96	158.5
42	B	339.48	201.3
42	i	275.87	144.9
42	r	227.69	164.7

TABLE II: This table shows the fluxes of STF 1169 AB and STF 42 AB in each filter used to take our images. The signal to noise ratios for these images were calculated from these values.

FIG. 4: The toolbar that appears when opening AstroImageJ. This toolbar can be used to open images and select the aperture tool used to measure the right ascension and declination of each star in a binary.

photographic approach to measuring the separation and position angle. Two of the images' properties were checked before any measurements were made in AstroImageJ: first, the image files were not labelled by filter, so the filter of each image was checked through the image header in FITS Liberator; then the image was uploaded into AstroImageJ where we could check if the image had been plate solved or not. The LCO automatically plate solved each image so we did not have to do the plate solving ourselves.

To calculate the current separation and position angle for STF 1169 AB and STF 42 AB, we calculated these values for each image individually and then averaged them; this can be done using the aperture tool in AstroImageJ. After opening AstroImageJ, a toolbar will appear − selecting *File->Open* and choosing a file will open the chosen image in a separate window with its own toolbar. In order to use the aperture tool on this image, the aperture radius must be set. The aperture size can be changed by then hovering over the *Edit* menu on the image toolbar and selecting *aperture settings*. This will open a third window in which you can you can change the *Radius of object aperture*. In the same window, make sure the box for *centroid apertures* is checked; this makes sure that when you use the aperture tool, it will snap to the center of the selected star automatically. Hit *OK* on the aperture window to save your settings; these settings should carry over to each new image you open so that you do not have to reset the aperture every time [5]. For our measurements, an aperture of 7 was used for every image of STF 1169 AB; for STF 42 AB a miscommunication occurred and different apertures were chosen for different sets of images. For the Bessel B and SDSS r' images an aperture of 4 was chosen, where as for the Bessel V and SDSS i' images, an aperature of 7 and 5 was used for the A star and B star respectively. Despite the miscommunication, the results for the STF 42 AB images were consistent, so we did not make new measurements with different apertures.

The aperture tool can be opened from the AstroImageJ toolbar seen in Figure 4; the icon for the tool is a blue dot surrounded by a red circle. Once the tool is selected drag the cursor over the A star in the image and click; this creates an automatically centered red circle around the star. After the star is selected, a pop-up window containing various measured values of the star will appear. Repeating the aperture tool process for the B star will cause its measurements to appear in the same pop-up as star A. Included in these measurements are the right ascension and declination of each star, the values we used to calculate the separation and position angle [5]. To make these calculations, we copy and pasted the measured values into an Excel sheet and use the following equations:

$$dRA = 15 * (RA(B) - RA(A)) * COS(RADIANS(DEC(B))) \quad (5)$$

$$dDEC = DEC(B) - DEC(A) \quad (6)$$

$$SEP = SQRT((dRA)^2 + (dDEC)^2) * 3600 \quad (7)$$

$$PA = DEGREES\left(ATAN\left(\frac{dRA}{dDEC}\right)\right). \quad (8)$$

Equations 5 and 6 give the change in right ascension and declination. These values can then be plugged into Equations 7 and 8 to give the separation and position angle. All of these calculations can be made in Excel by replacing *RA*, *DEC*, *dRA*, and *dDEC* with their appropriate Excel cell IDs [5].

After using the above process to calculate the separation and position angle for each image, we then took the average of these values for every filter using the Excel average function,

$$= AVERAGE(value\ 1 : value\ 2). \quad (9)$$

To take the average, replace *value* 1 and *value* 2 with the Excel cell IDs for the first and last values in the columns for separation and position angle. Then, using the same equation, we took the average of the average values for each filter; this produced a single value for the separation and position angle of the binary star. This process was done for both STF 1169 AB and STF 42 AB individually.

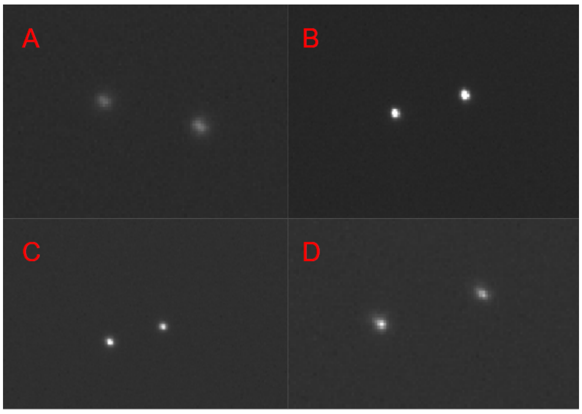

FIG. 5: Images of STF 1169 AB as seen in AstroImageJ. The images coincide to the following filters: A) Bessel B; B) Bessel V; C) SDSS r'; D) SDSS i'.

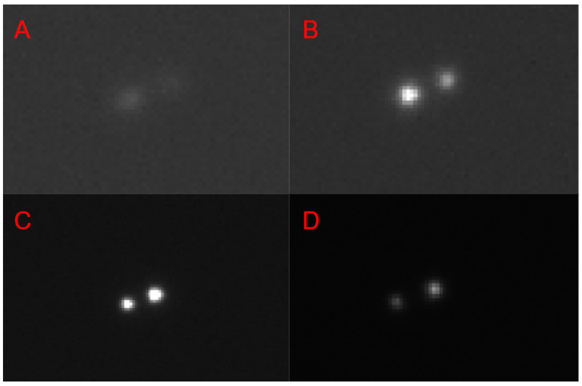

FIG. 6: Images of STF 42 AB as seen in AstroImageJ. The images coincide to the following filters: A) Bessel B; B) Bessel V; C) SDSS r'; D) SDSS i'.

III. RESULTS

The images of STF 1169 AB and STF 42 AB taken through the LCO telescopes can be seen in Figure 5 and Figure 6. As shown in both figures, the images taken in Bessel B and SDSS i' were the least clear, especially for the STF 42 AB Bessel B image, in which the B star is barely visible. This would have created more error when measuring the right ascension and declination of the stars. The images for STF 1169 AB in Bessel B have a different orientation than those of the other filters; this did not appear to affect our measurements of the right ascension and declination and was most likely due to the LCO telescope orientation when they were taking the images.

STF 1169 AB Separation & Postion Angle (Bessel B)		
Image #	SEP (arcsec)	PA (deg)
1	21.02962037	14.82907711
2	21.16747835	14.86780391
3	21.09634988	14.86412929
4	21.07153148	14.41235621
5	21.14349919	14.58233799
6	21.19271665	14.62985391
7	21.152438	14.52035633
8	20.89620536	15.06537853
9	21.06985297	14.74482697
10	21.02969856	14.44170222
11	21.10023257	14.7510048
12	20.99477581	14.85375239
13	20.97805028	14.00578514
14	21.14098829	14.74900861
15	21.12212508	14.23915789
STDEV	0.081273	0.276633
STD Error	0.020985	0.071426
Average	21.07904	14.6371

TABLE III: Table of the separation and position angle of STF 1169 AB calculated from 15 images taken in the Bessel B filter. Included in the table are the standard deviation, standard error, and average values for the separation and position angle.

STF 1169 AB Separation & Postion Angle (Bessel V)		
Image #	SEP (arcsec)	PA (deg)
1	20.75074	14.94954
2	20.68814	14.9958
3	20.72076	15.25346
4	20.74568	14.89704
5	20.74244	15.32166
6	20.75809	15.25363
7	20.85388	15.01385
8	20.76118	14.94185
9	20.66288	15.04285
10	20.69387	15.24559
11	20.7564	15.19861
12	20.81125	15.07345
13	20.81657	15.01338
14	21.01225	14.84191
15	20.82167	15.06563
STDEV	0.084787	0.147201
STD Error	0.021892	0.038007
Average	20.77305	15.07388

TABLE IV: Table of the separation and position angle of STF 1169 AB calculated from 15 images taken in the Bessel V filter. Included in the table are the standard deviation, standard error, and average values for the separation and position angle.

STF 1169 AB Separation & Postion Angle (SDSS r')		
Image #	SEP (arcsec)	PA (deg)
1	20.75959	14.88684
2	20.63625	14.92135
3	21.16053	16.39225
4	21.09665	16.66636
5	21.0722	16.5463
6	20.97782	16.67934
7	20.56713	15.28496
8	20.70235	14.87256
9	21.17709	16.26804
10	21.03772	16.57447
11	20.69255	14.96437
12	20.95934	16.75062
13	20.71183	14.89372
14	20.70901	14.98038
15	20.66543	15.06919
STDEV	0.211898	0.82405
STD Error	0.054712	0.212769
Average	20.8617	15.71672

TABLE V: Table of the separation and position angle of STF 1169 AB calculated from 15 images taken in the SDSS r' filter. Included in the table are the standard deviation, standard error, and average values for the separation and position angle.

STF 1169 AB Separation & Postion Angle (SDSS i')		
Image #	SEP (arcsec)	PA (deg)
1	21.11097	16.38504
2	21.13246	16.47914
3	21.17046	16.44897
4	20.9803	16.77026
5	21.02071	16.62502
6	21.01301	16.52001
7	21.1055	16.47293
8	21.21532	16.27476
9	21.08332	16.40694
10	21.06625	16.56053
11	21.02762	16.61949
12	21.03517	16.58551
13	21.17179	16.39225
14	21.09583	16.45303
15	20.69625	14.92542
STDEV	0.120903	0.424033
STD Error	0.031217	0.109485
Average	21.06166	16.39462

TABLE VI: Table of the separation and position angle of STF 1169 AB calculated from 15 images taken in the SDSS i' filter. Included in the table are the standard deviation, standard error, and average values for the separation and position angle.

STF 42 AB Separation & Postion Angle (Bessel B)		
Image #	SEP (arcsec)	PA (deg)
1	6.134937	20.99629
2	6.341314	19.83252
3	6.306774	21.7645
4	6.243299	21.99722
5	6.511425	20.60703
6	6.203269	22.14675
7	6.443348	23.5298
8	6.367634	21.99923
9	6.015635	22.39328
10	6.383747	21.48898
11	6.393876	20.55534
12	6.461935	22.10868
13	6.423966	21.34789
14	6.29427	22.26928
15	6.360303	21.57208
STDEV	0.13186145	0.89924497
STD Error	0.03404648	0.23218405
Average	6.32571547	21.6405913

TABLE VII: Table of the separation and position angle of STF 42 AB calculated from 15 images taken in the Bessel B filter. Included in the table are the standard deviation, standard error, and average values for the separation and position angle.

STF 42 AB Separation & Postion Angle (Bessel V)		
Image #	SEP (arcsec)	PA (deg)
1	6.22628881	20.2140826
2	6.18239252	20.3639481
3	6.25332283	20.1229036
4	6.24994269	20.1342573
5	6.23980379	20.1683929
6	6.20264702	20.2945146
7	6.21953271	20.2369996
8	6.3032942	20.4094935
9	6.26789681	19.619581
10	6.18239249	20.3639472
11	6.19589453	20.3176091
12	6.22628888	20.2140845
13	6.24318322	20.1570033
14	6.22628875	20.2140813
15	6.29163947	19.5425253
STDEV	0.0360237	0.25049577
STD Error	0.00930128	0.06467773
Average	6.23405391	20.1582282

TABLE VIII: Table of the separation and position angle of STF 42 AB calculated from 15 images taken in the Bessel V filter. Included in the table are the standard deviation, standard error, and average values for the separation and position angle.

STF 42 AB Separation & Postion Angle (SDSS r')		
Image #	SEP (arcsec)	PA (deg)
1	6.266845	20.0776
2	6.367445	20.19485
3	6.254334	19.66387
4	6.270227	20.06631
5	6.213671	19.79791
6	6.256703	20.11156
7	6.208175	19.35803
8	6.260084	20.10023
9	6.253323	20.1229
10	6.244165	19.69722
11	6.266846	20.0776
12	6.334518	19.85404
13	6.279682	20.48967
14	6.267897	19.61958
15	6.239804	20.16839
STDEV	0.04040558	0.28781995
STD Error	0.01043268	0.07431479
Average	6.26558127	19.959984

TABLE IX: Table of the separation and position angle of STF 42 AB calculated from 15 images taken in the SDSS r' filter. Included in the table are the standard deviation, standard error, and average values for the separation and position angle.

STF 42 AB Separation & Postion Angle (SDSS i')		
Image #	SEP (arcsec)	PA (deg)
1	6.21497934	19.3363231
2	6.24756652	19.6863888
3	6.29729849	19.9767081
4	6.23401009	19.7309734
5	6.28038451	20.032809
6	6.18320746	19.8999064
7	6.1899779	19.8772188
8	6.20013542	19.8432816
9	6.22292261	20.2258342
10	6.20690858	19.8207254
11	6.21368258	19.7982155
12	6.20013563	19.8432868
13	6.20352194	19.8319989
14	6.22630073	20.2143806
15	6.20013564	19.8432871
STDEV	0.03222992	0.21256097
STD Error	0.00832173	0.05488301
Average	6.22141116	19.8640892

TABLE X: Table of the separation and position angle of STF 42 AB calculated from 15 images taken in the SDSS i' filter. Included in the table are the standard deviation, standard error, and average values for the separation and position angle.

All 15 calculations of separation and position angle for each filter and binary star can be seen in Tables III through X. As well as the measurements, the standard deviation and standard error were calculated and included in the tables. The standard deviation was calculated with the Excel function listed below.

$$= STDEV(value\ 1 : value\ 2) \tag{10}$$

The standard error can be found by dividing the standard deviation by the square-root of the number of measurements made and was calculated using the following Excel function:

$$= STDEV(value\ 1 : value\ 2)/ \\ SQRT(COUNT(value\ 1 : value\ 2)) \tag{11}$$

As with Equation 9, Equations 10 and 11 can be performed in Excel by replacing *value* 1 and *value* 2 with the first and last cell IDs of the Column of data under analysis.

For the separation calculations of STF 1169 AB, the standard deviation was less than 0.3 *arcsec* in all filters; the highest standard deviation was 0.21 *arcsec* from the SDSS r' image, while the smallest standard deviation occurred in the Bessel B image at a value of 0.08 *arcsec*. The standard error for the separation did not go higher than 0.06 *arcsec*, with the largest error being 0.055 *arcsec* (SDSS r') and the smallest error being 0.022 *arcsec*. Given these values, we determined that all of the calculated values of STF 1169 AB's separation were within a reasonable error.

In terms of STF 1169 AB's position angle, the standard deviations and errors were higher in all filters than for the separation. The standard deviation reached a maximum of 0.82° in the SDSS r' filter and a minimum of 0.15° in the Bessel V filter. On the other hand, the standard error ranged from 0.21° in the SDSS r' image to 0.038° in the Bessel V image. Although they were larger than the position angle measurements, these values indicated that the measurements had a small enough error.

For both the separation and position angle of STF 1169 AB, the SDSS r' filter's image were the greatest source of error. In both measurements, the Bessel filters produced the smallest error.

Final Measurement of STF 1169 AB		
Filter	SEP (arcsec)	PA (deg)
B	21.07904	14.6371
V	20.77305	15.07388
r	20.8617	15.71672
i	21.06166	16.39462
STDEV	0.15063952	0.767158
STD Error	0.07531976	0.383579
Average	20.9438625	15.45558

TABLE XI: This table includes the averaged values of the separation and position angle of STF 1169 AB for each filter used. The average of these values is at the bottom of this table, along with its standard deviation and position angle.

Table XI shows the averaged values of the separation and position angle from each filter combined for STF 1169 AB, which came out to be 20.94 *arcsec* and 15.45°. The standard deviation and standard error for both values were low enough for the measurements to be deemed reasonable, but the errors in the position angle were higher than that of the separation. This could be due to a miscommunication in which star is the A or B star; in Equations 5 and 6, it does not matter which values for the right ascension and declination are subtracted first as long as it is consistent between both equations, but Equation 5 has a dependency on the *cos* of the declination of the B star. This factor changes depending on which star is selected as the B star and could change the values of dRA calculated. It was not discussed which star should be considered the A and B star, so it is likely that some measurements were made with the A and B stars backwards. The factor of dRA is used in both the separation and position angle expressions but it is possible that this error affected the position angle more.

STF 1169 AB Historical Data		
Year	SEP (arcsec)	PA (deg)
1832.35	20.74	10.1
1900.35	20.82	11.5
1930.19	20.913	12.8
1947.27	20.8	13.8
1962.227	20.692	14.962
2018.973	20.56	15.13
2022	20.94	15.5

TABLE XII: The first six values listed are historical measurements of STF 1169 AB's separation and position angle (provided by the WDS) and the last measurement included is the one made in this project. The historical data set included dozens of observations; these six were chosen as they represented the beginning of the time period in which the each particular position angle was most common. For example, starting in 1930 a position angle of about 14° was most common.

Our measurements for STF 1169 AB also fit the orbital trend established by past observations. As seen in Table XII, the binary system's separation has remained relatively constant since its first measurement in 1832; this is likely due to the stars large orbital period. On the other hand, STF 1169 AB's position angle has increased steadily since 1832, with its last measurement – prior to ours – being in 2018 and having a position angle of 15.13°. The measured position angle from this project, 15.5°, agrees with the prior measurement.

The standard deviations and errors for STF 42 AB's measurements are similar to that of STF 1169 AB. STF 42 AB's separation had standard deviations no greater than 2 *arcsec*; the highest standard deviation was in the Bessel B filter at 0.13 *arcsec*, while the lowest was at 0.032 *arcsec* in the SDSS i' filter. Its standard error for the separation had a maximum of 0.034 *arcsec* in the Bessel B filter and a minimum of 0.0083 *arcsec* in the SDSS i' filter. The higher degree of error in the B filter is likely due to how faint the second star is as seen in Figure 6; this would have made it difficult for AstroImageJ to select the same or near-the-same centroid for the second star in each image. Despite this, we considered the error to be small enough.

STF 42 AB's position angle calculations also had a higher standard deviation and error compared to its separation, which is again considered to be a consequence of not choosing the same A and B star for each measurement. The highest standard deviation came from the Bessel B images with a value of 0.90°, whereas the smallest standard deviation was produced by the SDSS i' filter and had a value of 0.21°. Bessel B and SDSS i' gave the highest and lowest standard error respectively with values of 0.23° and 0.054°. Again these errors were determined to be low enough.

The Bessel B filters produced the worst error in the data set for both the separation and position angle of STF 42 AB, while SDSS i' gave the best results in each case. Bessel B's poor performance is, again, most likely due to the poor visibility of the second star in its images.

Final Measurement of STF 42 AB		
Filter	SEP (arcsec)	PA (deg)
B	6.32571547	21.6405913
V	6.23405391	20.1582282
r	6.26558127	19.959984
i	6.22141116	19.8640892
STDEV	0.0465494	0.83230682
STD Error	0.0232747	0.41615341
Average	6.26169045	20.4057232

TABLE XIII: This table includes the averaged values of the separation and position angle of STF 42 AB for each filter used. The average of these values is at the bottom of this table, along with its standard deviation and position angle.

The finalized measurements of STF 42 AB's separation and position angle can be found in Table XIII, which are 6.26 *arcsec* and 20.41°. As expected, the standard deviation and error for the position angle are greater than for the separation, but both sets of errors are small enough for the data to be considered reasonable.

STF 42 AB Historical Data		
Year	SEP (arcsec)	PA (deg)
1824.88	6.55	33.7
1895.92	5.56	28.3
1948.71	5.76	25.6
1984.877	6.120	22.879
2015.632	6.2838	20.945
2020.74	6.037	20.82
2022	6.26	20.41

TABLE XIV: The first six values listed are historical measurements of STF 42 AB's separation and position angle (provided by the WDS) and the last measurement included is the one made in this project. The historical data set included dozens of observations; these six were chosen as they represented the beginning of the time period in which the each particular position angle was most common. For example, starting in 1948 a position angle of about 22° was most common.

We can again compare our data to the historical data by referring to Table XIV. As with STF 1169 AB, STF 42 AB's separation has held constant since its initial calculation in 1824. The position angle has increased periodically over time and has consistently been at around 20° for the last seven years. STF 42 AB's last measurement was made two years ago in 2020; our measurements of the separation and position angle are approximately equal to the prior measurements made, suggesting that STF 42 AB has not progressed much along its orbit. This is again likely due to STF 42 AB's large orbital period.

IV. DISCUSSION

Since our values of separation and position angle for both STF 1169 AB and STF 42 AB were consistent with both the historical trend and the latest measurement prior to our own, we can – for now – say that both binary stars are following the estimated orbital plots. Despite the accuracy of our data though, due to the long orbital periods of STF 1169 AB and STF 42 AB, it will take many more years before these estimated orbits can be considered accurate. As seen in Figures 1 and 2, the historical measurements span relatively short arcs of the estimated orbits despite including nearly two centuries worth of observations. For STF 1169 AB, the B star orbits in a counter-clockwise direction; if we had been able to insert our data point into this plot, it would appear on the outer edge of the pink, photographic data points. On both plots for STF 42 AB, the B star orbits in a clockwise direction and our data point would have appeared just after the blue, interferometric data points going in the same direction.

It was our intention going into this project to include our data points in a plot along with the historical data. We attempted to do this using the Excel *Plot Tool 3.19* developed by Richard Harshaw, but were unable to do so due to missing information; the plotting tool required information of the double stars that we did not have and failed to retrieve from the Gaia DR2 database suggested by Harshaw [8]. Another attempt was made to make a simple scatter plot of the data in Excel, but the plots generated provided no meaningful information on the double stars' orbits. This method most likely also required the information mentioned by Harshaw that we could not access. Therefore, since we could not graphically compare our data to the historical data, we chose to present a small portion of the historical data as a table so that the binary stars' progression could be seen visually. Gaining access to the missing Gaia DR2 data, though, would have helped us to analyze our data more effectively.

A potential way to make our data more accurate would be to directly measure the separation and position angle in AstroImageJ. In our haste to process our images, we used Equations 5 through 8 from a tutorial website with the intent of finding a scientific paper for them at a later date. While searching for this scientific source, we discovered that there was a way to make our measurements directly in the AstroImageJ program, but we had already calculated all of our data by that point and did not have time to redo it. The process of measuring the separation and position angle in AstroImageJ is simple; using the same aperture tool and settings, click on the A star and drag the mouse to the B star. Once the click is released, the aperture is automatically centered for both stars and a new pop-up window appears with the separation and position angle already calculated [2]. It is likely that this process uses the same equations as listed in this paper, but it would have been much more efficient to let AstroImageJ do the calculations for us.

Other changes that would be beneficial to our procedure would be selecting a standard aperture to use in every measurement for a given double and designating which star is the B star before making any measurements. Although it did not seem to affect the output of right ascension and declination measurements, a potential source of error could have been our irregular use of aperture size, specifically for STF 42 AB. Standardizing a specific aperture size across all filters could have created more accurate results for us to work with.

As discussed above, we did not state beforehand which stars were the A and B stars, causing our calculation of the change in right ascension, dRA, to have some deviation between filters. The differences in the declinations of the A and B star were small enough that these deviations were not noticeable and could potentially be considered negligible. Still it would be good practice to make sure we use the same star as the B star in future measurements so as to decrease any error it may have caused. Of course, if we were to use AstroImageJ to directly measure the separation and position angle, we would be able to skip this step entirely.

With the Gaia DR2 data and us now knowing how to measure the separation and position angle in AstroImageJ with proper aperture settings, we should be able to produce more accurate and usable results for future observations of STF 1169 AB and STF 42 AB or any other binary stars we may observe in the future.

V. ACKNOWLEDGMENTS

This research has made use of the Washington Double Star Catalog maintained at the U.S. Naval Observatory. This work makes use of observations from the Las Cumbres Observatory global telescope network.

---

[1] Aitken, R.G. "What We Know About Double Stars." *Royal Astronomical Society.* 13, May 1932.

[2] Badami, U.A., Tock, K., Carpenter, S., Kruger, K., Freed, R., & Genet, R.M., "Measurement of the Position Angle and Separation of HJ 1924." JDSO, vol. 14, no. 1, Jan. 2018, pp. 181-189.

[3] Brown, T.M., Baliber, N., Bianco, F.B., Bowman, M., Burleson, B., COnway, P., Crellin, M., Depagne, E., De Vera, J., & Dilday, B., "Las Cumbres Observatory Global Telescope Network." The Astronomical Society of the Pacific, 2013.

[4] Cahill, J., Boysen, Z., Clark, M., Wagner, G., & Tock, K., "Comparison and CCD Measurements of Four DOuble Star Systems: WDS 03003+1432, 03009+5221, 03001+3911, 08165+7930." JDSO, vol. 14, no. 4, Oct. 2018, pp. 694-704.

[5] "Double Stars Measurements With AstroImageJ." Astrojolo, 27 Aug. 2020.

[6] Dugan, L., Mizrachi, R., Boyarski, R., & Tock, K., "STF 42 AB Measurement and Reclassification." JDSO, vol. 28, no. 4, Oct. 2022, pp. 357-363.

[7] "Finding Our Place in the Cosmos: From Galileo to Sagan and Beyond."*Library of Congress.*

[8] Harshaw, R., "Using Plot Tool 3.19 to Generate Graphical Representations of the Historical Measurement Data." JDSO, vol. 16, no. 4, Sept. 2022, pp. 386-400.

[9] Heintz, W.D., "Double Stars."*Springer Science & Business Media.* 2012.

[10] Hughes, A., McNerney, M., Chung, S., Rendon, R., Ewing, J., & Harshaw, R., "Astrometry of WDS 09000-4933." JDSO, vol. 16, no. 2, Apr. 2020, pp. 169–72.

[11] Kisselev, A.A., Romanenko, L.G., & Kalinichenko, O.A., "A Dynamical Study of 12 Wide Visual Binaries." Astronomicheskii Zhurnal, vol. 86, no. 2, pp. 148-157.

[12] Latham, D.W., Mazeh, T., Carney, B.W., McCrosky, R.E., Stefanik, R.P., & Davis, R.J., "A Survey of Proper-Motion Sars VI. Orbits for 40 Spectroscopic Binaries." The Astronomical Journal, vol. 96, no. 2, Aug. 1988, pp. 567-587.

[13] Newton, C., Anderson, D., Morales, R., Gerow, T., Ramirez, B., Whipp, P., Rowe, D., Freed, R., & Genet, R., "CCD Observation of STF1169AB." JDSO, vol. 14, no. 1, Jan. 2018, pp.168-171.

[14] Tokovinin, A.A., "New spectroscopic components in 8 multiple systems." Astronomy & Astrophysics Supplement Series, ser. 136, 1999, pp. 373-378.

[15] Wirth, G.D.,"Astronomical Magnitude Systems." Harvard.